

Contents lists available at [SciVerse ScienceDirect](http://www.sciencedirect.com)

Energy

journal homepage: www.elsevier.com/locate/energy

The application of CFD modelling to support the reduction of CO₂ emissions in cement industry

Hrvoje Mikulčić^{a,*}, Milan Vujanović^a, Dimitris K. Fidaros^b, Peter Priesching^c, Ivica Minić^d, Reinhard Tatschl^c, Neven Duić^a, Gordana Stefanović^d

^a Faculty of Mechanical Engineering and Naval Architecture, University of Zagreb, Ivana Lučića 5, 10000 Zagreb, Croatia

^b Centre for Research and Technology-Thessaly, Institute of Technology and Management of Agricultural ecosystems, Technology Park of Thessaly, 1st Industrial Area of Volos, 38500 Volos, Greece

^c AVL – AST, Hans List Platz 1, Graz, Austria

^d Faculty of Mechanical Engineering, University of Niš, Aleksandra Medvedeva 14, 18 000 Niš, Serbia

ARTICLE INFO

Article history:

Received 30 August 2011

Received in revised form

23 March 2012

Accepted 9 April 2012

Available online xxx

Keywords:

Calcination process

Cement calciner

Cement industry

CO₂ emission

Energy efficiency

ABSTRACT

The cement industry is one of the leading producers of anthropogenic greenhouse gases, of which CO₂ is the most significant. Recently, researchers have invested a considerable amount of time studying ways to improve energy consumption and pollutant formation in the overall cement manufacturing process. One idea involves dividing the calcination and clinking processes into two separate furnaces. The calcination process is performed in a calciner while the clinking process takes place in a rotary kiln. As this is new technology in the cement manufacturing process, calciners are still in the research and development phase. The purpose of this paper is to demonstrate the potential of CFD to support the design and optimization of calciners, whose use appears to be essential in reduction of CO₂ emission during cement production. The mathematical model of the calcination process was developed, validated and implemented into a commercial CFD code, which was then used for the analysis. From the results obtained by these simulations, researchers will gain an in-depth understanding of all thermo-chemical reactions in a calciner. This understanding can be used to optimize the calciner's geometry, to make production more efficient, to lower pollutant formation and to subsequently reduce greenhouse gas emissions.

© 2012 Elsevier Ltd. All rights reserved.

1. Introduction

The cement industry has a significant effect on the environment. It is responsible for 5% of the world's anthropogenic CO₂ emissions, and therefore it is an important sector for CO₂ mitigation strategies [1,2]. Around 50% of CO₂ emissions produced during the cement manufacturing process come from the thermal decomposition of limestone, also known as the calcination process. Additionally, 40% comes from the combustion process [3]. CO₂ emission mitigation options include various process and combustion efficiency improvements. One of these improvements comes from controlling the calcination process during the cement production process. Calcination is a strong endothermic reaction, during which limestone

(CaCO₃) thermally decomposes into lime (CaO) and carbon dioxide (CO₂). In addition to the influence on cement quality, calcination also affects fuel consumption and pollutant emissions [4]. One possibility for the control and investigation of the calcination process is a Computational Fluid Dynamics (CFD) simulation. Early comprehensive information, parametric studies and initial conclusions that can be gained from CFD simulations are very important in handling modern cement technology requirements. Together with experiments and theory, CFD has become an integral component of calciner research. It has been used in the development process for understanding the complex phenomena occurring within the calcination and combustion processes. For instance, results gained from CFD simulations of the calcination process in the calciner can be used for the optimization of a calciner design. The result is a calciner with a higher performance. This higher performing calciner will then have an influence on the final cement quality, fuel consumption and pollutant emissions.

With the aim of understanding all chemical reactions, the heat exchange processes and fluid flow, different cement calciners have been studied. Fidaros et al. [4] presented a numerical model and

* Corresponding author. Tel.: +385 1 6168 494; fax: +385 1 6156 940.

E-mail addresses: hrvoje.mikulcic@fsb.hr (H. Mikulčić), milan.vujanovic@fsb.hr (M. Vujanović), dfeid@cereteth.gr (D.K. Fidaros), peter.priesching@avl.com (P. Priesching), ivica.minic@gmail.com (I. Minić), reinhard.tatschl@avl.com (R. Tatschl), neven.ducic@fsb.hr (N. Duić), goca@masfak.ni.ac.rs (G. Stefanović).

a parametric study of flow and transport phenomena that take place in an industrial calciner. This work shows good prediction capabilities for velocity, temperature and distribution of particles. Iliuta et al. [5] investigated the effect of different operating conditions on the level of calcination, burn-out and NO_x emissions of an in-line low NO_x calciner. This work made a sensitivity analysis of the model with respect to aerodynamics, combustion and calcination parameters. Huanpeng et al. [6] studied the impact of various physical parameters on the dynamics of the two-phase flow in a precalciner. This work used the kinetic theory of granular flow to represent the transport properties of the solid phase in a 2D model. Hu et al. [7] used a 3D model for a dual combustor and precalciner. An Eulerian frame was used for the continuous phase and a Lagrangean frame for the solid phase. The burn-out and the decomposition ratio during the simultaneous injection of two types of coal and limestone were predicted. Bluhm-Drenhaus et al. [8] studied the heat and mass transfer related to the chemical conversion of limestone to lime in a shaft kiln. CFD was used to model the transport of mass, momentum and energy in the continuous phase, while the discrete element method (DEM) was used to model the mechanical movement and the conversion reactions of the solid materials. Using a cement calciner in the cement production process is relatively new technology. Consequently, all of these studies show the need for further improvements of cement calciners.

In addition to studies investigating the chemical and physical processes in cement production, several studies investigated the potential of CO₂ emission reduction. In general, CO₂ emissions due to fossil fuel combustion in cement production systems can be reduced by using more energy efficient technologies in the existing production process [9,10]. Fidaros et al. [3] showed a parametric analysis of a solar calciner, using CFD as a research tool. The study also showed how CO₂ emissions can be decreased because the required heat comes from solar energy. Therefore, fossil fuels are not needed for the calcination process. Koumboulis and Kouvakas [11] demonstrated their dynamically adjustable controller for calciner exhaust gases, showing that, with a controlled calciner outlet temperature, the desirable precalcination degree can be achieved. They also showed that the corresponding energy consumption can be lowered according to the fuel used for the process. Kääntee et al. [12] investigated the use of alternative fuels in the cement manufacturing process. This research provided useful data for optimizing the manufacturing process by using different alternative fuels with lower calorific value than those used in classical configurations. Gartner [13] studied clinker chemistry to lower CO₂ emissions. This study showed that raw materials other than limestone could be used in cement production in order to reduce CO₂ emissions.

Due to the significance of the cement industry sector and increased environmental awareness [14], several studies, in different parts of the world, have demonstrated the energy efficiency of cement plants and CO₂ emissions reduction. Much of this work studied the improvement of the cement production process and options for CO₂ emission reduction. Pardo et al. [15] demonstrated the potential for improvement in energy efficiency of EU's cement industry and CO₂ emission reduction by the year 2030. Liu et al. [16] reported the potential for the renovation and building of new cement plants in China. Hasanbeigi et al. [17] demonstrated the abatement CO₂ cost curve for the Thai cement industry. The possibilities and costs of CO₂ abatement were identified, while considering the costs and CO₂ abatement for different technologies. Worrell et al. [18] presented an in-depth analysis of the US cement industry, showing the possibilities for energy saving and CO₂ emissions reduction, based on a detailed national technology database. This work emphasized that the most energy efficient

pyroprocessing cement manufacturing systems consist of preheaters, a calciner and a rotary kiln. Sheinbaum and Ozawa [19] reported the energy use and the CO₂ emissions in the Mexican cement industry, concluding that the focus of the energy and CO₂ emissions reduction should be on the use of alternative fuels. Szabó et al. [20] for the 2000–2030 period, presented the most important trends in world cement production, technology development and CO₂ emissions. The study showed that the most advanced dry-precalciner technologies are expected to be the most widely used by 2030. In addition, their work showed that global CO₂ emissions from the cement industry will increase by 50%.

The purpose of this paper is to present the potential of CFD-based CO₂ emission reduction in a Croatian cement plant. The best available technology for cement production, a dry rotary kiln together with preheating of the raw material and a cement calciner were used. In addition to the calculation of the CO₂ emission, a mathematical model of the calcination process was developed, validated and implemented into a commercial CFD code [21]. This calcination model was then used for numerical simulation of a specific calciner geometry which is reported in the literature [4].

1.1. Modern cement pyroprocessing unit

Fig. 1 illustrates the four main cement production processes which have the most influence on final cement quality and fuel consumption. These four processes are: raw material preheating, calcination, clinker burning, and clinker cooling [4]. Prior to the raw material preheating, the raw material is collected, crushed, mixed with additives and transported to the cyclone preheating system. Cyclone preheating systems (usually 3–4 cyclones) have been developed to improve the heat exchange process. Preheating occurs prior to the calciner and the rotary kiln, and has several stages. In every stage the principle is the same – raw material is moving

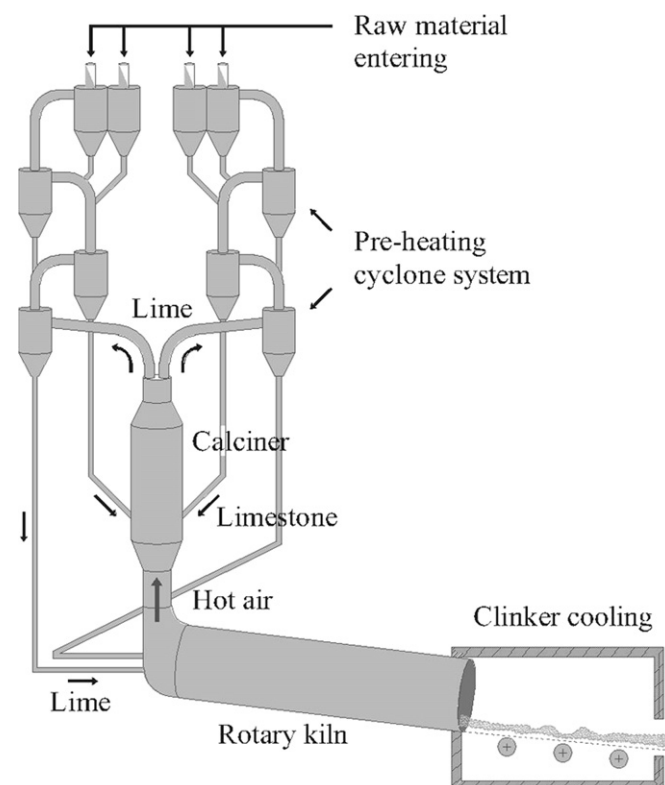


Fig. 1. General pyroprocessing unit of a cement production plant.

counter to hot exhaust gasses from the rotary kiln and in that way is heated. This process is repeated until the raw material goes through all cyclones.

After preheating, raw material enters the cement calciner, where the calcination process occurs. According to Szabó et al. [20] a decrease of energy consumption by 8–11% can be achieved when a rotary kiln is used together with a calciner. This decrease is due to the fact that cement calciners have lower temperatures than rotary kilns. To ensure a temperature of 850 °C, needed for a stabile calcination process, cement calciners use heat from the combustion of solid fuels along with the exhaust gases from a rotary kiln [22]. This is new technology in cement production. Therefore, cement calciners are not standard equipment in cement plants.

Clinker burning is the highest energy demanding process in cement production. It occurs after the calcination process. The clinker is produced in a rotary kiln which rotates 3–5 times per minute, and is positioned at an angle of 3–4°. This angle causes the material to slide and tumble down through the hotter zones towards the flame. The temperature of 1450 °C ensures the clinker formation. After the clinkering process in the rotary kiln is finished, the cement clinker is rapidly cooled down to 100–200 °C [23]. This process is done rapidly to prevent undesirable chemical reactions.

2. Theoretical background

2.1. Analytical calculation of CO₂ emissions

The analytical calculation of CO₂ emission was performed for a cement plant in Croatia. This particular cement plant uses a dry rotary kiln along with the preheating of the raw material in cement production. A calciner is not used at this plant. However, the plant operator is planning to increase the cement production while decreasing the CO₂ emissions. To ensure both criteria are satisfied, the plant operator is planning on modernizing the pyroprocessing unit and including a calciner. For that reason, the CO₂ emissions were calculated for a plant with and without a calciner. CO₂ is emitted from two different sources: the combustion of fossil fuels and the calcination process of limestone in which the clinker forming process also emits CO₂. The former refers to combustion CO₂ emissions, and the latter refers to process CO₂ emissions. Combustion CO₂ emissions are calculated on the basis of the fuel consumption [24]:

$$m_{\text{CO}_2(\text{combustion})} = m_{\text{fuel}} \times H_d \times e_{\text{fuel}} \times O_x \quad (1)$$

Process CO₂ emissions, originating from the conversion of the raw material, are calculated on the basis of the produced cement clinker:

$$m_{\text{CO}_2(\text{clinker})} = m_{\text{clinker}} \times e \times f \quad (2)$$

Table 1 shows the analytically calculated CO₂ emissions for this particular cement plant. From these results, it is clear that most of the CO₂ emissions come from the calcination process. Also, it should be noted that the amount of CO₂ coming from the calcination process cannot be reduced. CO₂ must be released during the calcination process ($\text{CaCO}_3 \rightarrow \text{CaO} + \text{CO}_2$). Thus, the major potential

for the reduction of CO₂ emissions will be in the design of the combustion processes (with or without a calciner).

As mentioned previously, CO₂ emissions can be reduced if a calciner is used prior to the rotary kiln [4,18,20]. In that case, a decrease of fuel consumption by 8–11% can be gained [20]. This means that with the reduction of the fuel consumption an overall reduction of 3–4% in CO₂ emissions (see Table 1) can be achieved.

2.2. Numerical simulation of a cement calciner

2.2.1. Mathematical model

To model a calciner, the decay of limestone to lime via release of carbon dioxide and the process providing the reaction enthalpy, e.g., the pyrolysis of pit coal to carbon and volatiles with subsequent heterogeneous oxidation of the carbon must be treated. The motion of solid particles is traced through the cement calciner by the Lagrangian formulation. The gas phase is solved by an Eulerian formulation [25]. The mathematical models for the calcination and combustion are treated in the Lagrangian spray module. The thermo-physical properties of the limestone, the lime and the components of the pit coal particles were entered into the commercial CFD code FIRE via user-functions [26–28]. The functions were written in the FORTRAN programming language. In general, the thermal decomposition of limestone into lime and carbon dioxide can be presented by the following equation:



Calcination occurs when the partial pressure of carbon dioxide in the ambient gas is lower than the decomposition pressure of limestone. The decomposition pressure p_{eq} and the chemical reaction rate k_{ch} defined by Silcox et al. [29] are:

$$p_{\text{eq}} = 4.137 \times 10^{12} \exp\left(-\frac{20474}{T}\right) \text{ [Pa]}, \quad (4)$$

$$k_{\text{ch}} = k_D (p_{\text{eq}} - p_{\text{CO}_2}) \text{ [mol m}^{-2}\text{s}^{-1}], \quad (5)$$

where p_{CO_2} is a partial pressure of carbon dioxide at the limestone reacting surface and

$$k_D = 1.22 \exp\left(-\frac{4026}{T}\right) \times 10^{-5} \text{ [mol m}^{-2}\text{s}^{-1}\text{Pa}^{-1}]. \quad (6)$$

Based on equations (4)–(6), the chemical reaction rate of the calcination process can be written as [21]:

$$k_{\text{ch}} = 5.0 \cdot 10^7 \exp\left(-\frac{24500}{T}\right) - 1.22 \cdot 10^{-5} \exp\left(-\frac{4026}{T}\right) p_{\text{CO}_2} \cdot \frac{A_{\text{por}}}{A_{\text{geom}}} \text{ [mol m}^{-2}\text{s}^{-1}], \quad (7)$$

where the effects of temperature, partial pressure of CO₂ and surface porosity are taken into account.

The physical reaction rate k_{ph} in the calcination process is defined as [30]:

$$k_{\text{ph}} = \frac{12 D_{\text{eff}} \cdot \text{Sh}}{R_{\text{CO}_2} d_{\text{part}} \bar{T}} \cdot p_{\text{ref}} \text{ [kg m}^{-2}\text{s}^{-1}], \quad (8)$$

taking into account the diffusion limitations of limestone.

The total reaction rate of the calcination process is the combination of the physical and the chemical reaction rate, and is represented as [31]:

Table 1

CO₂ emissions from a cement plant without and with a calciner.

Type of CO ₂ emissions	Without a calciner	With a calciner
Process emissions [tCO ₂ per annum]	241 000	241 000
Combustion emissions [tCO ₂ per annum]	166 000	149 500–153 700
Total CO ₂ emissions [tCO ₂ per annum]	407 000	390 500–394 700

$$k = \left[\frac{1}{k_{ph}} + \frac{1}{\eta \cdot \bar{k}_{ch}} \right]^{-1} \quad [\text{kg m}^{-2} \text{s}^{-1}], \quad (9)$$

where \bar{k}_{ch} is the chemical reaction rate in $[\text{kg m}^{-2} \text{s}^{-1}]$ and η is dimensionless pore efficiency factor.

The coefficient η is described in the following equation [32]:

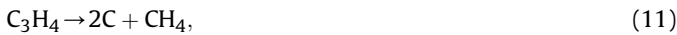
$$\eta = \frac{\tanh \left[\frac{d}{6} \sqrt{\frac{\bar{k}_{ch}}{D_{eff}}} \right]}{\left[\frac{d}{6} \sqrt{\frac{\bar{k}_{ch}}{D_{eff}}} \right]}, \quad (10)$$

where \bar{k}_{ch} is the chemical reaction rate in $[\text{s}^{-1}]$.

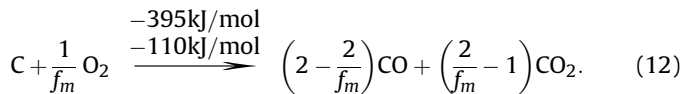
The presented mathematical model of the calcination process was thoroughly tested and validated in our previous studies. For quantitative checks of balances, the presented mathematical model was tested on a single particle [21]. Results gained from the single particle tests show that the decomposition of limestone depends on the following achieving reasonable trends: CO_2 content, the right range of temperatures, and the reaction kinetics of the calcination process. The mathematical model of the calcination process was validated by simulating the International Flame Research Foundation pipe reactor [21], for which measurements of limestone decomposition exist. Several experimental set-ups with different operating conditions have been calculated. This analysis gives more information about the impact of various parameters (CO_2 content, temperature, mass flow, etc.) on the calcination process.

For coal combustion, a two stage process is taken into account. Usually, complex chemistry systems in the FIRE solver are treated by pre-tabulation or similar methods [33]. In this case the coal combustion is a two stage process and is calculated directly. The coal particle, which is composed of pit coal and ash is undergoing a first stage pyrolytic decomposition into volatiles and pure carbon. In a subsequent step, treated in parallel to the pyrolysis, the carbon is oxidized to CO and CO_2 taking into account a mechanism factor depending on temperature.

For the pit coal, a very simple composition represented via chemical formula C_3H_4 is assumed. The heterogeneous chemical reactions treated for the basic model are:



and



Here, f_m denotes the so-called mechanism factor [34], which ranges between 1 and 2. It causes predominant production of CO_2 in the low temperature range below approximately 900 K and predominant generation of CO for higher temperatures. The value of f_m depends on the particle temperature and size.

Further, additional homogeneous reactions are treated inside the gaseous phase for the oxidation of CO [34] and the combustion of methane, which is treated via the four step Jones–Lindstedt mechanism [35]:

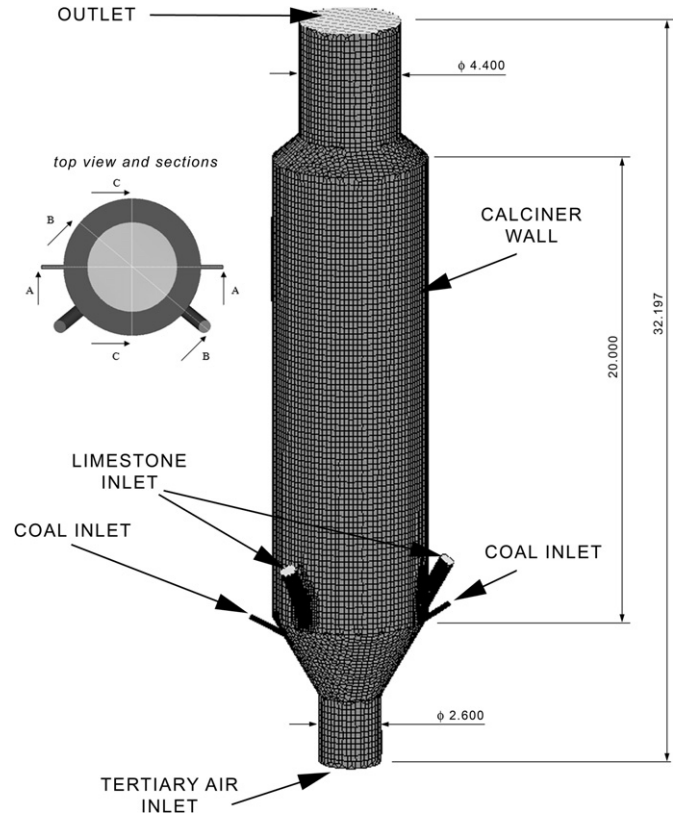


Fig. 2. Calciner boundary conditions and cross section views.



The homogeneous reactions inside the gaseous phase are treated within the general gas phase reactions module of the CFD code. The heterogeneous reactions cause mass transfer sinks and sources to the gas phase and particles. These are described by rate equations for pit coal consumption, for the carbon production from pyrolysis and for consumption from oxidation. As for the calcination, the total reaction rate is composed of a chemical rate following an Arrhenius approach and a physical rate introducing the rate limitation due to diffusion effects. Additional details of the model can be found in the literature [21].

2.2.2. Numerical simulation

The calciner geometry (Fig. 2), available in literature [4], was used to simulate the calcination process. The entire model is 32 m high, with three different cylinders and two conical sections connecting them. On the side of the calciner, there are two symmetric

Table 2
Initial conditions used for calciner calculation.

Pressure	0.1 [MPa]
Temperature	300 [K]
Gas composition	Air
Turbulent kinetic energy	0.001 [m^2/s^2]
Turbulent length scale	0.001 [m]

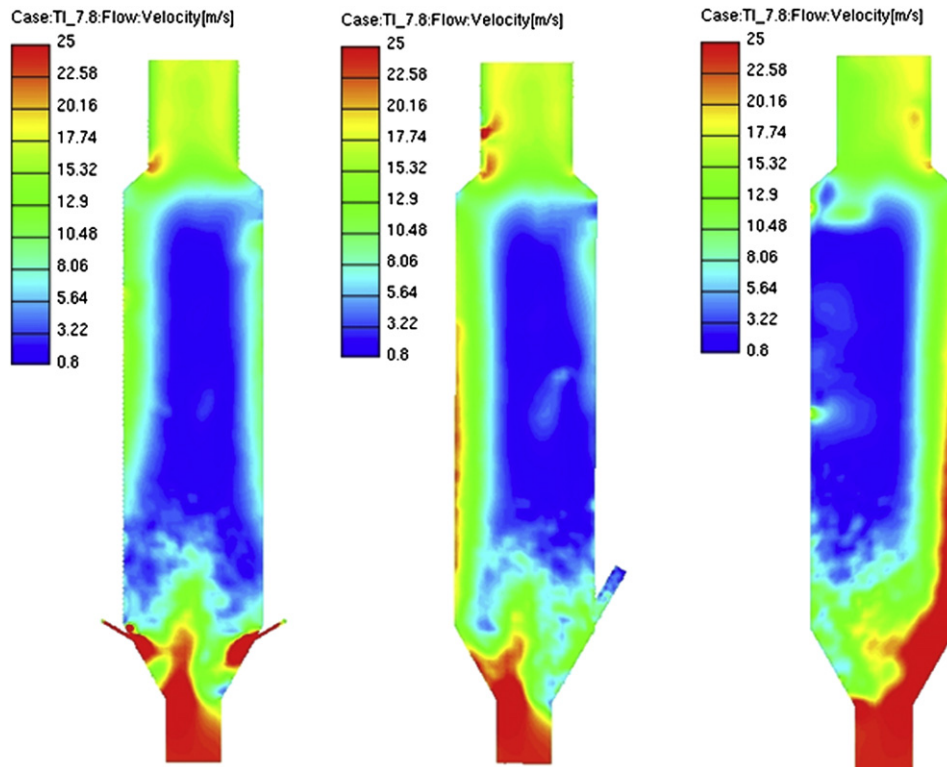


Fig. 3. Velocity distribution in vertical plane: section A-A (left); section B-B (middle); section C-C (right).

inlets for limestone. They are positioned at 60° angles and are 0.6 m in diameter. There are also two symmetric inlets for coal which are positioned at 30° angles and have a diameter of 0.2 m. The cylinder at the bottom of the calciner is 2.6 m in diameter and 3 m high. The

centre cylinder represents the main volume where physico-chemical reactions take place. It is 6.6 m in diameter and 20 m high. The cylinder at the outlet is 4.4 m in diameter and 4.7 high. The total volume of the calciner is 850 m^3 .

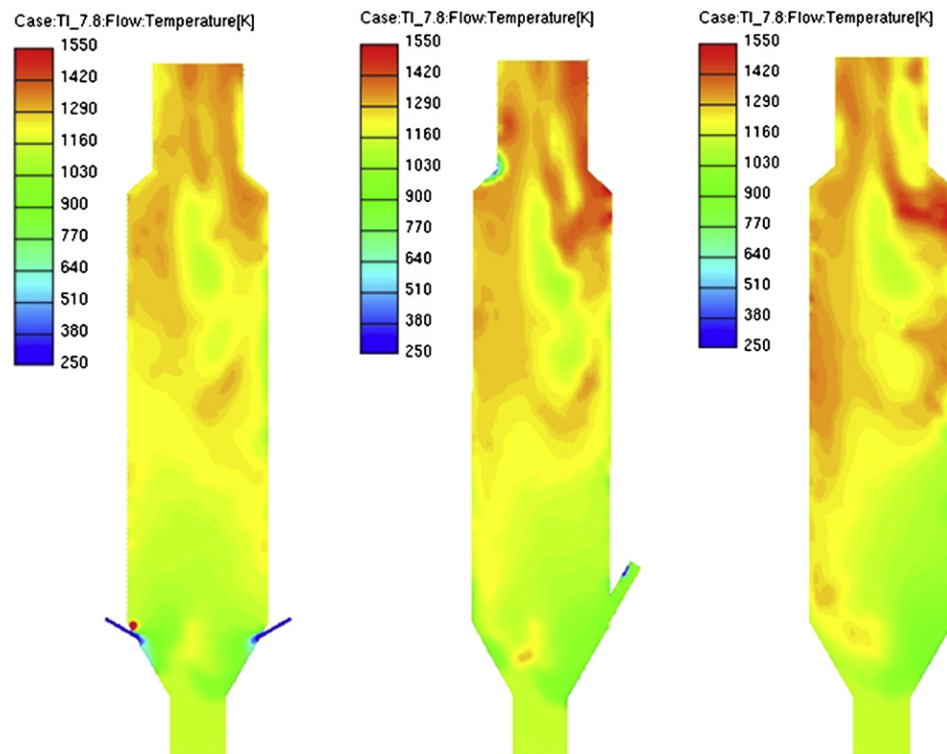


Fig. 4. Temperature field in vertical plane: section A-A (left); section B-B (middle); section C-C (right).

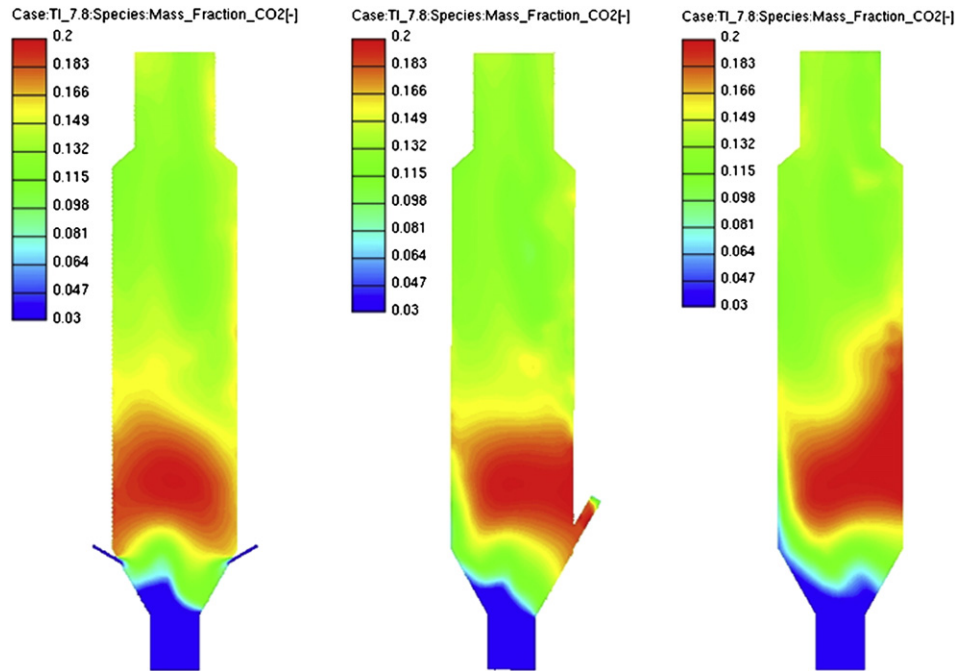


Fig. 5. CO₂ mass fraction in vertical plane: section A-A (left); section B-B (middle); section C-C (right).

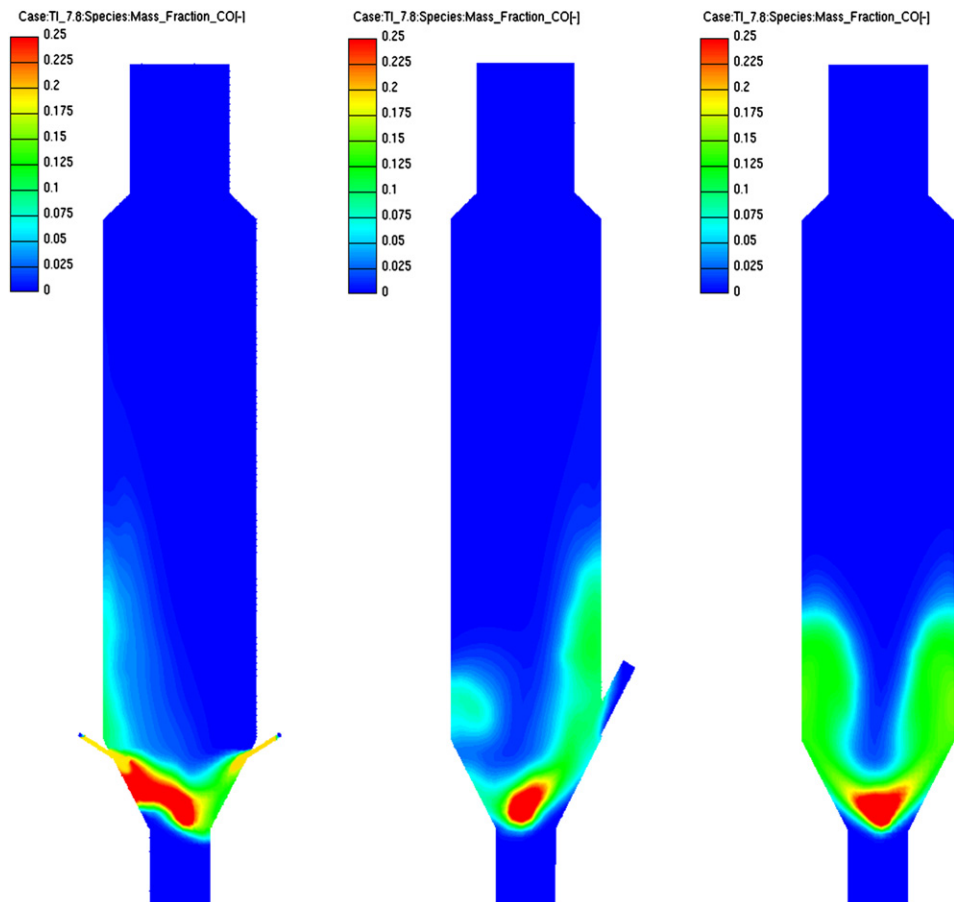


Fig. 6. CO mass fraction in vertical plane: section A-A (left); section B-B (middle); section C-C (right).

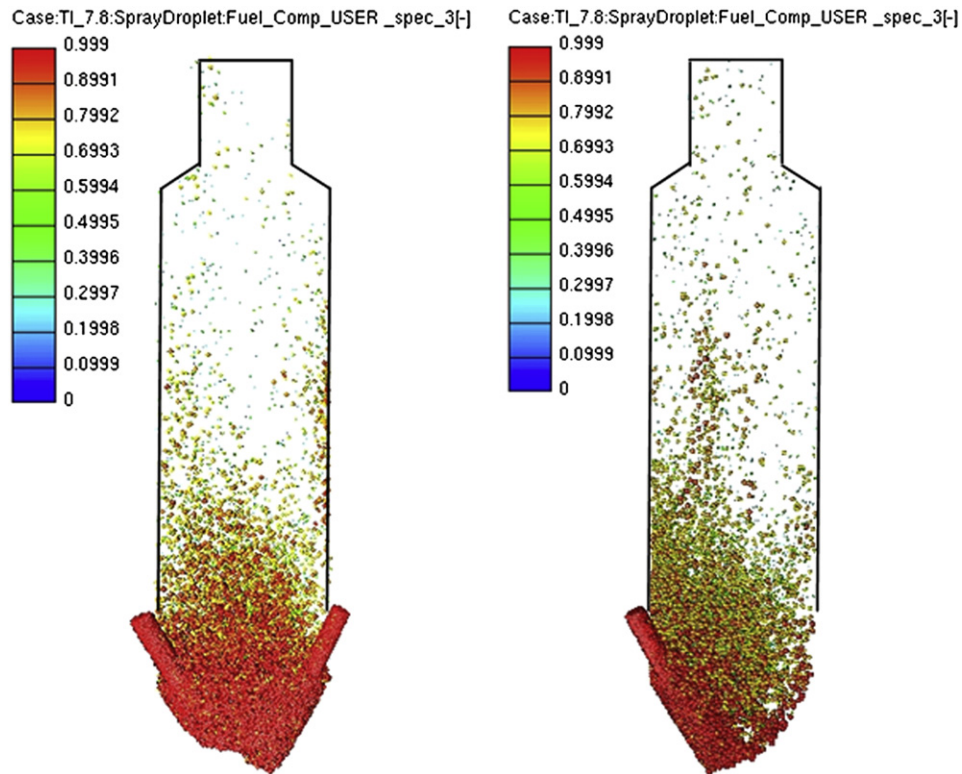


Fig. 7. Limestone (CaCO_3) particle: section A-A (left); section C-C (right).

The grid-size dependency for calcination calculation was analysed in our previous study [21]. Based on these results, 95 000 cells were employed to discretize the computational domain (Fig. 2) used in the simulation of the cement calciner. The calculation of the

values of variables at cell faces has a profound effect on the accuracy and the convergence, e.g., numerical stability, of the numerical method. For that reason, the differencing scheme used for momentum, continuity and enthalpy balances was MINMOD

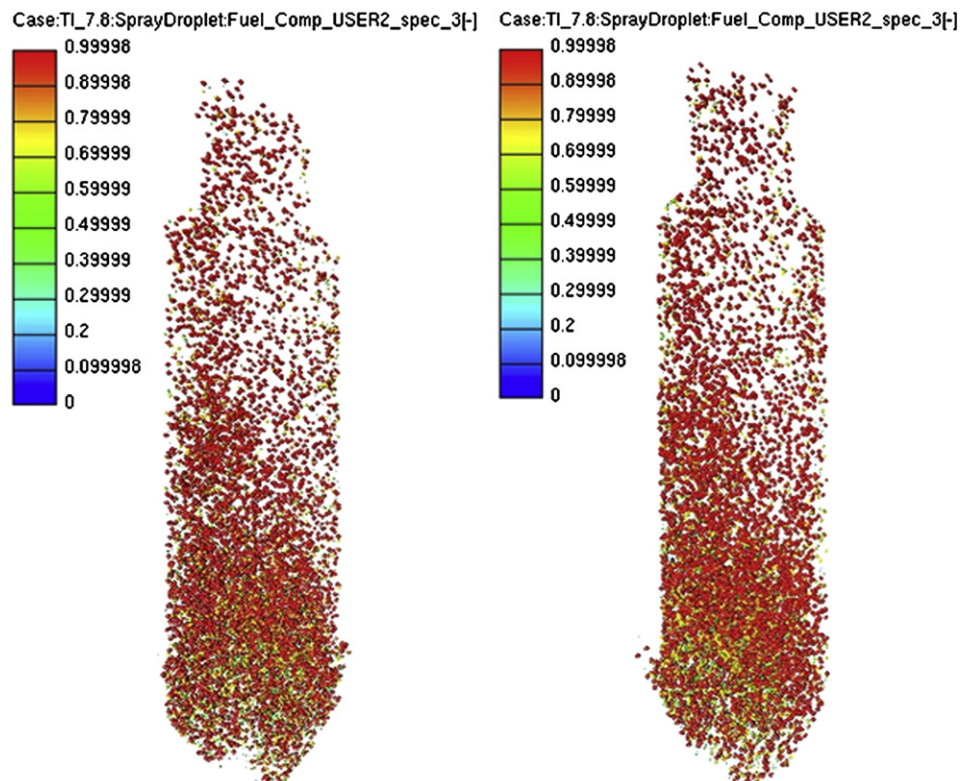


Fig. 8. Lime (CaO) particle: section A-A (left); section C-C (right).

Relaxed [36–38]. MINMOD Relaxed is a differencing scheme that combines advantages of the Upwind and the Central Differencing scheme. For the turbulence and scalar transport equations, an Upwind scheme was applied. The most favoured method for modelling turbulent flows in industrial applications is the Reynolds Averaged Navier–Stokes equations (RANS) with an appropriate turbulence model. Many turbulent models employ the concept of a turbulent viscosity or a turbulent diffusivity to approximate the turbulent Reynolds stresses and the turbulent heat fluxes. Turbulence was modelled by the standard $k-\epsilon$ model. This is the most widely used turbulence model in CFD simulations of practical engineering applications. It is numerically robust, offering a reasonable compromise between computational effort and accuracy, and it is generally accepted that the $k-\epsilon$ model yields reasonably realistic predictions of major mean-flow features in most situations [25,39]. For these reasons, the $k-\epsilon$ model is used in this work. The tertiary air entered the domain with the velocity of 24 m/s, limestone with 1.5 m/s, coal with 11.5 m/s, and static pressure of 10^5 Pa was used for the outlet boundary condition. The boundary conditions used for the calciner simulation are given in Fig. 2, and the initial conditions used for the calciner calculation are summarized in Table 2.

2.2.3. Results and discussion

Fig. 2 also shows the top view of the calculated calciner with the cross section views that are presented in the following figures.

Fig. 3 shows the velocity field in three different cross sections for the calculated cement calciner. In the central part of the calciner,

where the calcination reaction takes place, the velocity is around 3–5 m/s. As can be seen, a region with higher velocity occurs in the near wall region, and continues to the upper conical part and the outlet of the calciner. Section C–C clearly illustrates that the velocity in the region with the higher velocity is around 19–25 m/s, while in the middle of the calciner it is around 3–5 m/s. The main coal and raw material inlet are in the lower conical part of the calciner and from section C–C it can be seen that the velocity in that part of the calciner is around 20 m/s. The Reynolds number on the inlet of the tertiary air is around 3.5×10^5 .

Fig. 4 shows the temperature field in three different cross sections for the calculated cement calciner. As can be seen, the highest temperature occurs in the region where coal combustion is taking place. In that region, the average temperature is around 1200 °C. In the central part of the calciner, i.e. especially in the lower part and in the transition range to the combustion zone, where the limestone decomposition is taking place, the temperature is around 950 °C. This is the desirable temperature for the calcination process, slightly higher than the decomposition temperature of limestone, which ensures the process of calcination.

From Fig. 5 it is clear that the highest concentration of CO₂ is in the region where the decomposition of limestone is taking place, i.e. in the lower conical part of the calciner. It can also be seen that the concentration of CO₂ is decreasing towards the calciners outlet. This is due to the smaller limestone concentration.

Fig. 6 shows the concentration of CO in three different cross sections for the calculated cement calciner. It can be seen that the concentration of CO is highest in the lower part of the calciner. The

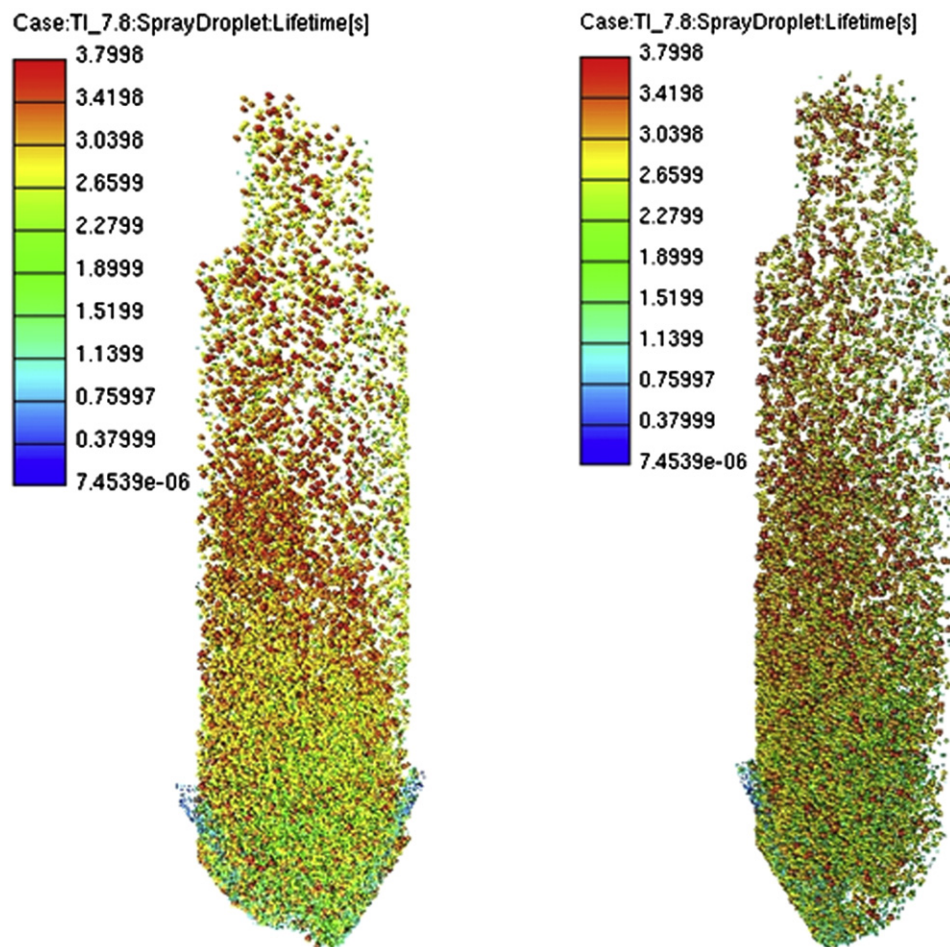


Fig. 9. Particle residence time section A-A (left); section C-C (right).

reason for this is the incomplete combustion of coal. It is harmful to have CO in the exhaust gases, however it can be seen that in the middle part of the calciner, CO further oxidises and forms CO₂.

Fig. 7 shows the portion of limestone in the entering raw material particle. Red represents 100% of limestone in the particle. The other colours represent a lower portion of limestone in the particle, with blue representing a fully decomposed limestone particle, i.e. a lime particle. For completeness, the overall contour of the limestone and lime particles is given. The 'empty' regions inside this contour indicate the regions where conversion, to a large extent, has already been completed. Also, it can be seen that the particles are carried with higher velocity, and consequently they are on one side of the calciner.

Fig. 8 shows the portion of lime in the entering raw material particle. Red represents 100% of lime in the particle, the rest of the colours represent a lower portion of lime in the particle. Also, from this figure it can be concluded that the particles are carried with the higher velocity, and consequently, they are mostly on one side of the calciner.

Fig. 9 shows the particle residence time. The coal particles are also shown. They are mainly located at the outer regions on the right side of the figure. It can be noted that the calculated residence time of both coal and lime/limestone particles is around 3.5 s.

There are no experimental data available for this calciner. Therefore, we could not compare the numerical predictions. However, validation of the calcination model, used for this calculation, was performed in our previous study [21]. The results achieved by this calculation demonstrate that the developed model for the calcination process [21] coupled with the commercial CFD code, is a suitable and promising tool for plant optimization. That was the focus of this study. Although the validation or the verification of a developed numerical model with experimental data is essential for such studies, it should be noted that the placement of the appropriate instrumentation for specific data recording and extraction (like fluid velocities components, peak spatial temperatures at high frequency rates) is not possible in fully operational devices. Also, for many reasons, related to production alteration rates and/or the altered fuel and raw material supply, the experiment's measurement repeatability is practically impossible under such conditions. Here it is worth noting that the measurement quantities acquired by the plant's measurement devices, motoring magnitudes like temperatures, fuel consumption, volumetric flows may, and should, be compared with the data provided by the simulations, as those data remain many times the only evidence in real working conditions.

The calcination process in a calciner is an energy saving process, which was also shown by the analytic calculation of CO₂ emissions. The cement calciner is supplied with appropriate quantity of fuel in order to achieve the calcination process. If this process takes place in the rotary cement kiln, the fuel supply should ensure that the main core temperature will exceed the 1450 or 1500 °C for length larger than 2/3 of total device in order to achieve firstly the calcination and then the clinkering process. The calcination process in a calciner is performed under significantly lower temperatures, approximately 850 °C, saving fuel and reducing the extra CO₂ which would be produced by extra fuel supply.

3. Conclusion

The CO₂ emissions created by the cement production systems have enhanced environmental concerns in the context of the present discussion on required CO₂ emission reduction efforts. From the analytical calculation of possible CO₂ reductions for a cement plant in Croatia, it is clear that a CO₂ emission reduction is possible by using a calciner prior to a rotary kiln. The present paper

demonstrates that CFD can serve as an advanced tool to analyse and improve the understanding of all thermo-chemical reactions occurring in real industrial configurations. This understanding can further on be used for the optimization of cement calciner's geometry and operating conditions. By optimizing its operating conditions, a reduction of fuel consumption can be achieved, resulting in the reduction of CO₂ emissions. The presented mathematical model is detailed enough to predict velocity, temperature, and all relevant physical and chemical processes needed for a CFD simulation of a cement calciner. From the results shown, it can be concluded that the physical expectations are well described with the presented mathematical model. Thus, the presented simulation method can be applied for the investigation and optimization of cement calciners in order to improve energy efficiency and reduce greenhouse gas emissions.

Nomenclature

$m_{\text{CO}_2(\text{combustion})}$	CO ₂ combustion emissions, t
m_{fuel}	fuel consumption, t
H_d	lower calorific value, TJ/t
e_{fuel}	fuel emission factor, tCO ₂ /TJ
O_x	oxidation factor, dimensionless
$m_{\text{CO}_2(\text{process})}$	CO ₂ clinker production, t
m_{clinker}	clinker production, t
e	emission factor, tCO ₂ /t
f	conversion factor, dimensionless
A_{geom}	sphere surface, m ²
A_{por}	overall reaction surface, m ²
D	diffusion coefficient, m ² s ⁻¹
k	overall reaction rate, kg m ⁻² s ⁻¹
d	particle diameter, m
T	temperature, K
\bar{k}_{ch}	chemical reaction rate, kg m ⁻² s ⁻¹
k_{ch}	chemical reaction rate, mol m ⁻² s ⁻¹
$\bar{\bar{k}}_{\text{ch}}$	chemical reaction rate, s ⁻¹
R_{CO_2}	CO ₂ gas constant, J kg ⁻¹ K ⁻¹
p_{CO_2}	CO ₂ partial pressure, Pa
p_{eq}	equilibrium CO ₂ partial pressure, Pa
d_{part}	particle diameter, m
k_{ph}	physical reaction rate, kg m ⁻² s ⁻¹
k_D	reaction rate, mol m ⁻² s ⁻¹ Pa ⁻¹
p_{ref}	referent pressure, Pa
Sh	Sherwood number, dimensionless
f_m	mechanism factor, dimensionless

Greek symbols

η	pore efficiency factor, dimensionless
--------	---------------------------------------

References

- [1] Stefanović G, Vučković G, Stojiljković M, Trifunović M. CO₂ reduction options in cement industry – the Novi Popovac case. *Thermal Science* 2010;14:671–9.
- [2] Cement Technology Roadmap. Carbon emission reduction up to 2050. Available at: International Energy Agency <http://www.iea.org/>; 2009 [accessed 2.2.2011].
- [3] Fidaros DK, Baxevanou CA, Vlachos NS. A parametric study of a solar calcinator using computational fluid dynamics. *Energy Conversion and Management* 2007;48:2784–91.
- [4] Fidaros DK, Baxevanou CA, Dritselis CD, Vlachos NS. Numerical modeling of flow and transport processes in a calciner for cement production. *Powder Technology* 2007;171:81–95.
- [5] Iliuta I, Dam-Johansen K, Jensen A, Jensen LS. Modeling of in-line low-Nox calciners – a parametric study. *Chemical Engineering Science* 2002;57: 789–803.
- [6] Huanpeng L, Wentie L, Jianxiang Z, Ding J, Xiujian Z, Huilin L. Numerical study of gas–solid flow in a precalciner using kinetic theory of granular flow. *Chemical Engineering Journal* 2004;102:151–60.

- [7] Hu Z, Lu J, Huang L, Wang S. Numerical simulation study on gas–solid two-phase flow in pre-calciner. *Communications in Nonlinear Science and Numerical Simulation* 2006;11:440–51.
- [8] Bluhm-Drenhaus T, Simsek E, Wirtz S, Scherer V. A coupled fluid dynamic-discrete element simulation of heat and mass transfer in a lime shaft kiln. *Chemical Engineering Science* 2010;65:2821–34.
- [9] Hayashi D, Krey M. Assessment of clean development mechanism potential of large-scale energy efficiency measures in heavy industries. *Energy* 2007;32:1917–31.
- [10] Akashi O, Hanaoka T, Matsuoka Y, Kainuma M. A projection for global CO₂ emissions from the industrial sector through 2030 based on activity level and technology changes. *Energy* 2011;36:1855–67.
- [11] Koumboulis FN, Kouvakas ND. Indirect adaptive neural control for precalcination in cement plants. *Mathematics and Computer in Simulation* 2002;60:325–34.
- [12] Kääntee U, Zevenhoven R, Backam R, Hupa M. Cement manufacturing using alternative fuels and the advantages of process modeling. *Fuel Processing Technology* 2004;85:293–301.
- [13] Gartner E. Industrially interesting approaches to “low-CO₂” cements. *Cement and Concrete Research* 2004;34:1489–98.
- [14] Vujanović M, Duić N, Galović A. Three-dimensional numerical simulation of the nitrogen oxides formation in an oil-fired furnace. *Strojarstvo* 2007;49:165–71.
- [15] Pardo N, Moya JA, Mercier A. Prospective on the energy efficiency and CO₂ emissions in the EU cement industry. *Energy* 2011;36:3244–54.
- [16] Liu F, Ross M, Wang S. Energy efficiency of China's cement industry. *Energy* 1995;20(7):669–89.
- [17] Hasanbeigi A, Menke C, Price L. The CO₂ abatement cost curve for Thailand cement industry. *Journal of Cleaner Production* 2010;18:1509–18.
- [18] Worrell E, Martin N, Price L. Potentials for energy efficiency improvement in the US cement industry. *Energy* 2000;25:1189–214.
- [19] Sheinbaum C, Ozawa L. Energy use and CO₂ emissions for Mexico's cement industry. *Energy* 1998;23(9):725–32.
- [20] Szabó L, Hidalgo I, Ciscar JC, Soria A. CO₂ emission trading within the European Union and annex B countries: the cement industry case. *Energy Policy* 2006;34:72–87.
- [21] Mikulčić H, von Berg E, Vujanović M, Priesching P, Perković L, Tatschl R, et al. Numerical modelling of calcination reaction mechanism for cement production. *Chemical Engineering Science* 2012;69(1):607–15.
- [22] BAT Guidance Note on Cement Industry, CARDS. Project further approximation of croatian legislation with the environmental acquis. Available at: <http://www.mzopu.hr/>; 2004 [accessed 17.8.2010].
- [23] Methodology for the free allocation of emission allowances in the EU ETS post-Sector report for the cement industry – Available at: http://ec.europa.eu/clima/studies/ets/benchmarking_en.htm; 2012 [accessed 27.1.2011].
- [24] [In Croatian]. Zagreb, Croatia Instructions for tracking and reporting of greenhouse gas emissions from the facility resulting from the activities listed in annex I of the regulation on greenhouse gas emission quotas and emissions trading; 2009.
- [25] Vujanović M. Numerical modeling of multiphase flow in combustion of liquid fuel. PhD-thesis, University of Zagreb, Zagreb, Croatia; 2010.
- [26] Baburić M, Duić N, Raulot A, Coelho PJ. Application of the conservative discrete transfer radiation method to a furnace with complex geometry. *Numerical Heat Transfer, Part A, Applications* 2005;48:297–313.
- [27] Baburić M, Raulot A, Duić N. Implementation of discrete transfer radiation method into SWIFT computational fluid dynamics code. *Thermal Science* 2004;8:293–301.
- [28] Vujanović M, Duić N, Tatschl R. Validation of reduced mechanisms for nitrogen chemistry in numerical simulation of a turbulent non-premixed flame. *Reaction Kinetics and Catalysis Letters* 2009;96:125–38.
- [29] Silcox GD, Kramlich JC, Pershing DW. A mathematical model for the flash calcination of dispersed CaCO₃ and Ca(OH)₂ particle. *Industrial Engineering Chemistry* 1989;28:155–60.
- [30] Schneider M. Experimentelle und mathematische Modellierung der Festbrennstoffvergasung am Beispiel der Gleichstromvergasung von Holzchackschnitzeln. PhD-thesis TU Dresden, Germany; 2003.
- [31] Levenspiel O. Chemical reaction engineering. 2nd ed. New York: J. Wiley and Sons; 1972. p. 482.
- [32] Froment G, Bischoff K. Chemical reactor analysis and design. 2nd ed. New York: J. Wiley and Sons; 1990. p. 160.
- [33] Ban M, Duić N. Adaptation of n-heptane autoignition tabulation for complex chemistry mechanisms. *Thermal Science* 2011;15:135–44.
- [34] Görner K. Technische Verbrennungssysteme, Grundlagen, Modelbildung, Simulation. Berlin, Heidelberg: Springer-Verlag; 1991.
- [35] Jones WP, Lindstedt RP. Global reaction scheme for hydrocarbon combustion. *Combustion and Flame* 1988;73:233–49.
- [36] FIRE_v2011_Manuals.
- [37] Harten A. High resolution schemes using flux limiters for hyperbolic conservation laws. *Journal of Computational Physics* 1983;49:357–93.
- [38] Harten A. High resolution schemes for hyperbolic conservation laws. *Journal of Computational Physics* 1991;49:225–32.
- [39] Blazek J. Computational fluid dynamics: principles and applications. Amsterdam, London, New York, Oxford, Paris, Shannon, Tokyo: Elsevier; 2001.